Research Square

Preprints are preliminary reports that have not undergone peer review.
They should not be considered conclusive, used to inform clinical practice,
or referenced by the media as validated information.

Webserver Integrated Machine Learning Platform for Predicting Polymer Imprinting Factors in Cancer Therapeutics

Meenakshy Krishnan PR
Amrita Viswa Vidyapeetham
Himadri Jadon
Manipal University Jaipur
Jisha R C
Amrita Viswa Vidyapeetham
Manjusha Nair
Amrita Viswa Vidyapeetham
Renuka Suravajhala
suravajhala.renuka@jaipur.manipal.edu
Manipal University Jaipur

Research Article

Keywords: Molecularly Imprinted Polymers (MIPs), Imprinting Factor (IF), Anticancer Drugs, Webserver, 3D Molecular Visualization, Drug-based MIP system

Posted Date: October 29th, 2026

DOI: https://doi.org/10.21203/rs.3.rs-11127093/v1

License: This work is licensed under a Creative Commons Attribution 4.0 International License.
Read Full License

Additional Declarations: No competing interests reported.

Abstract

Molecularly imprinted polymers (MIPs) is a class of synthetic receptors capable of specifically recognizing and binding target molecules by forming a molecularly defined binding site. These polymers have been known for its application in drug delivery, clinical diagnosis and biosensing. However, the design and optimization of MIP systems often require extensive experimental trial and error. In this work, we attempted to develop a webserver for the computational design, optimization, visualization of anticancer drug-based MIP systems. The platform enables the user to provide the molecular structures of the template anticancer drug, functional monomers, and crosslinkers in SMILES format, parameters such as the concentrations of template, monomers, crosslinker and monomer molecular weight. Users can customize the number of monomers and crosslinkers to develop virtually different polymer compositions and their predicted imprinting factor can be calculated. The webserver provides real-time three-dimensional visualization of the MIP polymer network interactions. Furthermore, we can predict the properties of bond-length distributions and binding-capacity estimations to analyze molecular interactions and structural characteristics of the designed systems. The imprinting factor (IF) of a molecularly imprinted polymer is predicted using a machine-learning based model as a parameter to evaluate the relative binding performance and selectivity of molecularly imprinted systems.

Scientific Contribution: Based on our previous machine-learning algorithm based study for predicting imprinting factors in molecularly imprinted polymers [https://doi.org/10.47852/bonviewJCCE62027832], this work integrates molecular structure based input, virtual polymer composition, three-dimensional structural visualization, binding-capacity assessment, and machine-learning-based prediction of the Imprinting Factor (IF) into a single web-based platform specifically designed for anticancer drug-based MIP systems. It enables the preliminary analysis and optimisation of the MIP formulations before experimental synthesis. We can integrate computational prediction to bridge the gap between conventional strategies and transform experimental optimization. By integrating machine learning based models relative binding efficiency and selectivity can be predicted. The developed webserver differs from conventional MIP optimization workflows. It provides data-driven support to rational optimization of preliminary design of anticancer drugs based MIPs.

Highlights

1. Computational framework for clustering of anticancer drug based Molecularly Imprinted Polymers (MIPs)
2. To analyze cavity features and support imprinting efficiency evaluation and the 3D visualization.
3. Predictive model for estimating the Imprinting Factor (IF) of Molecularly Imprinted Polymers (MIPs) which is designed for anticancer drug templates.
4. Input data form as SMILES of templates, monomers and crosslinkers for more than 100 types of FDA approved anticancer drugs along with binding capacity and bond length distribution analysis for every MIP visualization.

1. Introduction

One of the main causes for mortality is cancer, accounting for an estimated 19.3 million new cases in 2020 (Jemal et al., 2021). Surgery, chemotherapy and radiotherapy was set as a standard medication and protocol which have contributed remarkable outcomes for patient survival but are restricted because of severe side effects, incomplete selectivity towards malignant tumors along with systemic toxicity (Thurston, 2007; National Cancer Institute, 2019). Chemotherapeutic drugs in particular suffer from poor bioavailability, non-specific bio distribution, and the emergence of resistance, therefore this shows the need for better strategies in targeted drug delivery (Kaur et al., 2022; Tucker, 2019).

Anticancer drugs are widely classified into various classes, including antitubulin agents, antimetabolites, monoclonal antibodies, DNA-interactive agents, molecular targeting agents and also naturally derived product therapeutics shown in *Figure1* below along with *Table 1* which also includes the mode of action of various anticancer drugs (Thurston, 2007; Stringer & Snyder, 2007). While these agents use various mechanisms such as DNA cross-linking, microtubule destabilization or topoisomerase inhibition their clinical utility can be frequently achieved by dose-limiting toxicities and narrow therapeutic indices. Additionally, variability in patient pharmacodynamics (PD) and pharmacokinetics (PK) contributes to unpredictable efficacy and adverse effects (Stuurman et al., 2013).

S.No	Class	Example	Mode of action	References
1	Antimetabolites	Methotrexate	Disrupt the synthesis of nucleic acids	(D.E. Thurston, 2007)
2	Alkylating agents	Procarbazine	Introduces alkyl group into DNA.	(D.E. Thurston, 2007)
3	Crosslinking agents	Cisplatin	Binding to DNA resulting to an intra- strand or inter-strand cross-linking of DNA	(D.E. Thurston, 2007)
4	Intercalating agents	Doxorubicin	Binding between base pairs, inhibiting **topoisomerase II**, causing DNA damage and apoptosis.	(Donna S. Shewach and Robert D. Kutcha, 2008).
5	Topoisomerase inhibitors	Irinotecan	Drugs inhibit the responsible enzymes for the cleavage, annealing	(D.E. Thurston, 2007)
6	Antitubulin agents	Docetaxel	Interfere with microtubule dynamics, blocks cell division leads to cell death	(D.E. Thurston, 2007)

Table 1: Represents the classes of anticancer drugs, its mode of action

To overcome these challenges, various types of drug delivery systems (DDSs) have been developed, including solid lipid nanoparticles, liposomes, polymeric carriers and cyclodextrins (Mandal et al., 2021). These methods utilize the enhanced permeability and retention (EPR) effect and ligand-based active

targeting which helps in selectivity and therapeutic outcomes. Among all DDS (drug delivery systems), Molecularly Imprinted Polymers (MIPs) have emerged as promising candidates because they have high stability, structural fidelity, and capacity for selective recognition of target molecules (Zaidi et al., 2016; Bodoki et al., 2019). MIP-based drug delivery systems (DDSs) have shown potential in enhanced loading efficiency, controlled release of drugs at target sites and improved targeting in challenging physiological environments, making them particularly effective for anticancer therapy (da Silva et al., 2012; Paul et al., 2017).

Despite their ability, the rational design of anti-cancer based drugs specific to MIPs remains limited by the labor-intensive nature of optimization with experiments. Computational modeling and machine learning (ML) driven predictive approaches provide a powerful alternative which enables the rapid evaluation of binding specificity and Imprinting Factor (IF), these are some critical parameters for assessing efficiency of MIPs . Previous studies have shown the utility of ML models in predicting IF values for general MIP formulations, with Random Forest algorithms achieving superior performance (low RMSE, high accuracy) compared to other regression methods (Thurston, 2007). However, these models were not specifically optimized for anticancer drug based MIPs which leaves an important gap in translational applications.

In our previous study, machine learning models were designed to predict the imprinting factor (IF) of molecularly imprinted polymers based on the data set that includes 214 experimental observations with various combinations of template molecules, functional monomers, and crosslinkers [https://doi.org/10.47852/bonviewJCCE62027832]. Among the tested algorithms, Random Forest achieved an RMSE of 3.54, an MAE of 2.19, and an R^2 of 0.55. The results highlighted the potential of using machine learning algorithms as a preliminary tool to estimate the MIP binding performance. To facilitate the research process, a more accessible computational platform was proposed in the current study. By integrating molecular input, virtual polymer design, 3D structure visualization, binding capacity evaluation, and machine learning-driven IF prediction, a web-based platform was constructed to empower the researchers with an all-in-one solution.This present study addresses this gap by developing a multimodal computational framework and web server for anticancer drug based MIPs. The platform incorporates:

1. 3D visualization of drug, monomer and crosslinker interactions
2. Machine learning based Imprinting Factor prediction

2. Materials and Methodology

Monomers, Crosslinkers, and Templates: For the designing of Molecularly Imprinted Polymers (MIPs), the following chemicals were selected based on their functionality and compatibility with anticancer drugs, also the summary of main components and tools used in visualization is shown below in *Table 2*:

- Monomers : Methacrylic acid (MAA), Ascorbic acid, 4-vinylpyridine (4-VP)

- Crosslinkers: Ethylene Glycol Dimethacrylate (EGDMA), octane, Trimethylol propane trimethacrylate (TRIM)
- Templates: Doxorubicin, Lapatinib, Curcumin, Paclitaxel, Methotrexate, Sorafenib, Gefitinib, Irinotecan, Capecitabine, Etoposide, Docetaxel, Tegafur, 5-Fluorouracil, Procarbazine, Erlotinib, Crizotinib.

Software and Packages: Computational modeling and molecular visualization were done using Python (v3.9.21, Jupyter Notebook) by using packages like RDKit, Py3Dmol, NumPy, NetworkX, Matplotlib. Numerical computations were done using np. linalg.norm (), np. mean(), np.std(), Chem.SanitizeMol(mol), UFFGetMoleculeForceField(mol). Data Visualization was done using plt.hist(), plt.bar().

Component	Purpose	Software/Function used	Description or Parameters
Monomer	Polymer backbone formation	Chem.MolFromSmiles() (RDKit)	SMILES-based structure conversion
Crosslinker	Crosslinking agent	InsertMol() into RWMol (RDKit)	10 units inserted (can insert more number for a denser matrix)
Template	Imprint molecule	Chem.AddHs(), EmbedMolecule() (RDKit)	Hydrogen addition and ETKDG 3D optimization
3D optimization	Molecular conformer generation	AllChem.EmbedMolecule () (RDKit)	ETKDG algorithm used for realistic geometry
Bond length Analysis	Structural integrity verification	GetAtomPosition () + np.linalg.norm()	Distance measured between bonded atom pairs
Visualization	Molecular rendering	py3Dmol.view(), setStyle() (Py3Dmol)	Ball-and-stick, color-coded by molecule type
Plotting	Bond length distribution plot	matplotlib.pyplot	Frequency plot

Table 2: Summary of main components and tools used in Visualization

Data Collection: A total of 60 anticancer drugs were selected through an extensive literature review. Relevant pharmacological and physicochemical properties such as SMILES representations, bioavailability, toxicity profiles, and solubility data were collected for each drug from publicly available resources like DrugsBank, PubChem, and recent peer-reviewed studies. Based on a thorough literature survey, it was observed that 44 out of 60 anticancer drugs had no prior studies related to Molecularly Imprinted Polymer (MIP) based applications, while 16 anticancer drugs were studied with respect to

MIP-based applications. These 16 drug-based MIPs were considered for developing webserver-based visualization and image processing applications.

3D visualization of MIP polymer network construction:

- Monomers and crosslinkers were defined via SMILES and converted into 3D structures (Chem.MolFromSmiles). Hydrogen atoms were added (Chem.AddHs), and low-energy conformers were generated using AllChem.EmbedMolecule with Experimental - Torsion Knowledge Distance Geometry (ETKDG) algorithm which is a method used in RDKit to generate realistic 3D molecule conformations from 2D structures or smiles strings.
- A pre-polymerization assembly was simulated using 20 monomer units and 10 crosslinker units (Chem.RWMol).
- Template molecules were embedded into the polymer framework using InsertMol().
- Bond lengths between atoms were calculated using RDKit's conformer methods and NumPy and visualized as a histogram using Matplotlib to analyze structural integrity.

Template Binding MIP simulation: The binding of the template molecule to the polymer was modeled by inserting the template into the previously connected polymer matrix using InsertMol(). Following this, the combined complex was converted into MOL format using Chem.MolToMolBlock(). 3D visualization of the complete polymer-template system was performed using Py3Dmol, with monomer, crosslinker, and template atoms color-coded for clarity. This step confirmed correct spatial arrangement prior to template removal. The py3Dmol.view() function was used to render a ball-and-stick model of the complex.

Template Removal and Rebinding MIP simulation: Templates were computationally removed using RemoveAtom(), mimicking the washing step to generate Non-Imprinted Polymers (NIPs). The resulted polymer structure which now consists of only the monomers and crosslinkers was re-embedded in 3D space using AllChem.EmbedMolecule() with ETKDG algorithm and the structure was converted into MOL block format using Chem.MolToMolBlock() and visualized using Py3Dmol.

In the rebinding phase of simulation, the template molecule was reintroduced into the previously prepared Non-Imprinted Polymer (NIP) structure. A new editable molecule was created using Chem.RWMol(). The template was reinserted into the polymer matrix using InsertMol(). The complete polymer-template complex was then embedded into 3D space using AllChem.EmbedMolecule() to optimize its conformation. The resulting structure was converted into MOL format using Chem.MolToMolBlock() and Py3Dmol was used to render the polymer in a ball-and-stick model.

Binding and Rebinding Energy Calculations: The thermodynamic stability of polymer–template interactions was evaluated using the Universal Force Field (UFF) in RDKit using AllChem.UFFGetMoleculeForceField(). The total energy of each system was calculated using the

CalcEnergy() function. The binding energy (ΔEbinding) was calculated using: $\Delta E_{binding} = E_{complex} - (E_{polymer} + E_{template})$

Imprinting Factor (IF) was calculated as: IF = QMIP/ QNIP

where; QMIP is the Binding capacity of the imprinted polymer (μmol/g) and QNIP is the Binding capacity of the non-imprinted polymer (μmol/g). If IF>1, the MIP shows selective binding towards the template. The higher the IF value the better the imprinting efficiency of the polymer.

3. Results

To facilitate structural analysis of molecularly imprinted systems, an interactive 3D visualization module was created and integrated into a webserver built with Streamlit. The subsequent section describes the visual representations utilized in analyzing template binding, removal, and rebinding in the polymer matrix.

Visualization of Polymer-Template binding: A 3-D ball-and-stick representation of the polymer-template system was generated using Py3Dmol for understanding the binding efficiency of the polymer-template system. The template molecule (green) is seen as embedded within the polymer matrix, indicating successful pre-polymerization binding. The visualization for the drug Methotrexate shown in *Figure 2* confirmed the effective positioning of the template within the polymer matrix. Following polymerization, the template molecule was computationally removed from the polymer matrix. To evaluate the specificity of the generated cavities, the template molecule was reintroduced into the polymer matrix, revealing that the template has reoccupied the cavity regions formed during imprinting. This rebinding behavior demonstrates the structural recognition capability inherent to Molecular Imprinted Polymers (MIPs).

Template Rebinding Visualization: To evaluate the specificity of the generated cavities, the template molecule was reintroduced into the polymer matrix. This rebinding behavior demonstrates the structural recognition capability inherent to Molecular Imprinted Polymers (MIPs). Further validation of imprinting and rebinding were confirmed through the analysis of rebinding energies.

Binding and Rebinding Energy Analysis:

To evaluate the efficiency of molecular imprinting and the potential binding strength of anticancer drugs, binding and rebinding energies were calculated for 16-anticancer drugs MIP complexes in *Table 3*.

Drugs	Binding Energies (kcal/mol)	Rebinding Energies (kcal/mol)
Methotrexate	-160.48	-152.14
Docetaxel	-109.96	-136.88
Lapatinib	-107.34	-134.54
Doxorubicin	-104.28	-102.84
Paclitaxel	-90.45	-153.37
Irinotecan	-77.36	-99.61
Sorafenib	-67.20	-66.18
Etoposide	-41.81	-50.80
Tegafur	-41.04	-53.16
Crizotinib	-34.48	-31.87
Procarbazine	-18.13	-30.23
Curcumin	-19.37	-17.77
Capecitabine	-12.58	-13.15
5-Fluorouracil	-11.26	-17.17
Erlotinib	-8.34	-14.52
Gefitinib	-5.57	-11.93

Table 3: Represents Binding and Rebinding Energies of anticancer drugs

As demonstrated in Figure 3, the webserver provides system and simulation parameters that allow users to define and modify the conditions in the virtual MIP system. The system parameters can be customized specifically by the users related to the concentrations of the template, functional monomer, and crosslinker, the polymerization volume (L), and monomer molecular weight (g/mol). These parameters provide the composition and stoichiometry of the modeled MIP system. The simulation parameters allow the users to customize the number of monomers, crosslinkers to generate diverse virtual polymer compositions of monomer- crosslinker ratios and can optimize. Based on the selected parameters, the webserver generates a 3D representation illustrating the spatial arrangements of the modeled MIP system. 3D structures show information related to bond-length distributions and displayed to aid in the structural analysis of the modeled system. The platform offers binding-capacity calculations. Such web servers support predicting different polymer formulations, Visualizing structural and binding features.

4. Discussion

A webserver was implemented to enable users to input molecular structures in SMILES format for template drugs, functional monomers, and crosslinkers. The platform provides a real-time three-dimensional view of the modeled polymer-template complexes, which enables users to interpret the spatial distribution of the involved molecular entities and the predicted binding environment in the MIP system. An important aspect of the webserver is the calculation of the Imprinting Factor (IF) as a quantitative reference for comparing the relative binding performance of imprinted and non-imprinted systems. Thus, the IF can be applied as a computational parameter for preliminary comparison of the investigated MIP formulations.

A summary of the binding classification is presented in Table 4 with representative anticancer drugs from each category. According to the machine learning models that clustered the calculated binding and rebinding energy values, the modeled MIP complexes were divided into three groups of strong, intermediate, and weak binders for comparative interpretation. In the present study, anticancer drugs with a binding or rebinding energy below -100 kcal/mol were classified as strong binders, while those with a binding or rebinding energy of -100 and -50 kcal/mol were classified as intermediate binders. On the other hand, drugs with a binding or rebinding energy above -50 kcal/mol were classified as weak binders. The observed classification provides a relative reference for interpreting the calculated interaction energies of the investigated anticancer drugs, and this should not be considered as the experimentally proven binding-strength thresholds but can be designed based on assumptions. We are further developing the anticancer drug based MIPs based on webserver prediction.

The strong-binding group consisted of Docetaxel, Paclitaxel, and Doxorubicin, which were characterized by more negatively calculated binding/rebinding energies within the defined classification range. Sorafenib, Tegafur, and Etoposide were categorized as intermediate binders, while Erlotinib, Procarbazine, and Curcumin were categorized as weak binders. The observed dissimilarities can be attributed to variations in the size, functional group composition, polarity, and types and extent of interactions that can take place between the studied anticancer drug molecules and the modeled polymer environment.

Binding Strength	Anticancer Drugs
Strong	Docetaxel, Paclitaxel, Doxorubicin
Intermediate	Sorafenib, Tegafur, Etoposide
Weak	Erlotinib, Procarbazine, Curcumin etc.

Table 4: Classification of Anticancer drugs based on rebinding energy values

The comparative binding and rebinding energies of the 16 anticancer drugs are presented in Graph 1. More negative energy values are indicative of stronger calculated interactions within the applied computational model. The comparison of the binding and rebinding energies provides another means for evaluating the differential interaction pattern of the template molecules before and after the

computational rebinding process. The observed differences between the investigated drugs demonstrate that the computational framework can differentiate the predicted interaction strength within the modeled MIP systems.

However, the calculated binding and rebinding energies reflect computational estimates, which should not be interpreted as experimental measurements of the binding affinity, cavity stability, and selectivity. Simultaneously, the classification into strong, intermediate, and weak binders can be applied for comparative interpretation within the present computational analysis. The experimental synthesis, characterization, and binding/selectivity studies would be required to verify the predicted interaction patterns and determine whether the computationally identified systems possess the corresponding properties experimentally. Nevertheless, the combined analysis of the binding/rebinding energies and IF provides an opportunity for a preliminary comparison and screening of anticancer drug-based MIP formulations.

Conclusion

The developed webserver provides an integrated computational platform to design, visualize, and evaluate anticancer drug-based molecularly imprinted polymer (MIP) systems. The platform enables the user to input molecular structures of template drugs, functional monomers, and crosslinkers in SMILES format and define relevant system and simulation parameters to generate different virtual MIP compositions. The 3D visualization allows the user to visualize the spatial arrangement of the template, monomers, and crosslinkers and explore the interactions represented within the modeled polymer network. In addition, the platform offers bond-length distributions, binding-capacity calculations, binding and rebinding energy estimates, and machine-learning-based imprinting factor (IF) prediction for comparative evaluation of different MIP formulations.

The combination of structural visualization with quantitative computational analysis allows the user to screen and compare different combinations of anticancer drug templates, functional monomers, and crosslinkers before experimental synthesis. The platform can therefore be used as a complementary approach to conventional experimental optimization by enabling preliminary evaluation of different MIP formulations in silico. This can be especially valuable when comparing candidate monomers and polymer compositions for anticancer drugs with diverse molecular structures, functional groups, and physicochemical properties.

Limitations

The webserver predictions depend on the algorithms, scoring functions, input parameters, and datasets used to develop the model and therefore should be considered preliminary computational estimates. The predicted binding and rebinding energies, imprinting factors need to be experimentally validated. In addition, the webserver is limited by the relatively specific set of template molecules and functional monomers included in the dataset and is especially designed for anticancer drug-based MIPs. The

prediction performance may vary by about 10–15% accuracy depending on the input and training data. Therefore, an experimental synthesis and characterization are further required to verify the computational predictions as future perspectives.

Declarations

Data and Software Availability

The web server developed in this study is publicly accessible at [https://bioinformatics-if-prediction.streamlit.app/Visualization]. The web server enables prediction of the imprinting efficiency of molecularly imprinted polymers based on the user-provided molecular structures and polymerization parameters. The molecular structures, input parameters, and prediction results used in this study are available through the web server. The source code and additional data supporting the findings of this study are available at: [https://github.com/jishamenon1/bioinformatics/blob/main/Introduction.py], where applicable.

Authors' Contribution

Meenakshy Krishnan P R: Data collection, Methodology, Analysis, Visualization, Interpretation of data, Initial draft

Himadri Jadon: Analysis, Visualization, Initial draft

Jisha R C: Computational methodology, Technical support, Web server development, and critical review of the manuscript.

Manjusha Nair: Computational methodology, Technical support, Web server development, and critical review of the manuscript.

Dr. Renuka Suravajhala: Conceptualization, Supervision, Methodology, Interpretation of data, Draft Proofread.

Funding and Acknowledgement

We are thankful to the Manipal University Jaipur, Jaipur, Rajasthan, India for providing APC funding.

Ethics Approval and consent to participate

Not applicable to present study

Consent to Publish declaration

Not applicable

Competing Interest

The authors declare that they have no competing interests.

Clinical Trial Number

Not Applicable

References

1. Adhikari, H. S., & Yadav, P. N. (2018). Anticancer activity of chitosan, chitosan derivatives, and their mechanism of action. *International Journal of Biomaterials, 2018*, 2952085. https://doi.org/10.1155/2018/2952085
2. Akgönüllü, S., Kılıç, S., Esen, C., & Denizli, A. (2023). Molecularly imprinted polymer- based sensors for protein detection. *Polymers. 15*(3), 629. https://doi.org/10.3390/polym15030629
3. Almeida, A., Araújo, M., Novoa-Carballal, R., Andrade, F., Gonçalves, H., Reis, R. L., Lúcio, M., Schwartz, S., & Sarmento, B. (2020). Novel amphiphilic chitosan micelles as carriers for hydrophobic anticancer drugs. *Materials Science and Engineering: C, 112*, 110920. https://doi.org/10.1016/j.msec.2020.110920
4. Ansari, L., Derakhshi, M., Bagheri, E., Shahtahmassebi, N., & Malaekeh-Nikouei, B. (2020). Folate conjugation improved uptake and targeting of porous hydroxyapatite nanoparticles containing epirubicin to cancer cells. *Pharmaceutical Development and Technology, 25*, 601–609. https://doi.org/10.1080/10837450.2020.1725045
5. Arima, H., Hagiwara, Y., Hirayama, F., & Uekama, K. (2006). Enhancement of antitumor effect of doxorubicin by its complexation with γ-cyclodextrin in pegylated liposomes. *Journal of Drug Targeting, 14*(4), 225–232. https://doi.org/10.1080/10611860600711136
6. Arpicco, S., Dosio, F., Stella, B., & Cattel, L. (2011). Anticancer prodrugs: An overview of major strategies and recent developments. *Current Topics in Medicinal Chemistry, 11*, 2346–2381.
7. Bakshi, P. S., Selvakumar, D., Kadirvelu, K., & Kumar, N. S. (2020). Chitosan as an environment friendly biomaterial—A review on recent modifications and applications. *International Journal of Biological Macromolecules, 150*,1072–1083. https://doi.org/10.1016/j.ijbiomac.2019.10.113
8. Balogh, L. P. (Ed.). (2017). *Nanomedicine in cancer*. CRC Press.
9. Batlokwa, B., Mokgadi, J., Nyokong, T., & Torto, N. (2011). Optimal template removal from molecularly imprinted polymers by pressurized hot water extraction. *Chromatographia, 73*(7-8), 589–593. https://doi.org/10.1007/s10337-010-1884-3
10. Bedwell, T. S., & Whitcombe, M. J. (2016). Analytical applications of MIPs in diagnostic assays: Future perspectives. *Analytical and Bioanalytical Chemistry, 408*(7), 1735–1751. https://doi.org/10.1007/s00216-015-9137-9
11. Bhalla, N., Jolly, P., Formisano, N., & Estrela, P. (2016). Introduction to biosensors. Essays in Biochemistry, 60(1), 1–8. https://doi.org/10.1042/EBC20150001

12. Bhatia, D., Paul, S., Acharjee, T., & Ramachairy, S. S. (2024). Biosensors and their widespread impact on human health. Sensors International, 5, 100257. https://doi.org/10.1016/j.sintl.2023.100257
13. Bitas, D., & Samanidou, V. (2018). Molecularly imprinted polymers as extracting media for the chromatographic determination of antibiotics in milk. Molecules, 23(2), 316. https://doi.org/10.3390/molecules23020316
14. Blackburn, C., Sullivan, M. V., Wild, M. I., O'Connor, A. J., & Turner, N. W. (2024). Utilization of molecularly imprinting technology for the detection of glucocorticoids for a point of care surface plasmon resonance (SPR) device. Analytica Chimica Acta, 1285, 342004. https://doi.org/10.1016/j.aca.2023.342004
15. Buntin, M. B., Burke, M. F., Hoaglin, M. C., & Blumenthal, D. (2011). The benefits of health information technology: A review of the recent literature shows predominantly positive results. Health Affairs, 30(3), 464–471.
16. Cabaleiro-Lago, C., Hasterok, S., Gjörloff Wingren, A., & Tassidis, H. (2023). Recent advances in molecularly imprinted polymers and their disease-related applications. Polymers, 15(21),4199. https://doi.org/10.3390/polym15214199
17. Çetin, K., & Denizli, A. (2015). 5-Fluorouracil delivery from metal-ion mediated molecularly imprinted cryogel discs. Colloids and Surfaces B: Bio interfaces, 126, 401– 406.
18. Chen, Y., Yan, X., Zhao, J., Feng, H., Li, P., Tong, Z., Yang, Z., Li, S., Yang, J., & Jin, S. (2018). Preparation of the chitosan/poly (glutamic acid)/alginate polyelectrolyte complexing hydrogel and study on its drug releasing property. Carbohydrate Polymers, 191, 8–16. https://doi.org/10.1016/j.carbpol.2018.02.065
19. Cui, J., Li, C., Wang, C., Li, Y., Zhang, L., Xiu, X., & Wei, N. (2011). Development of pegylated liposomal vincristine using novel sulfobutyl ether cyclodextrin gradient: Is improved drug retention sufficient to surpass DSPE-PEG-induced drug leakage? Journal of Pharmaceutical Sciences, 100(7), 2835–2848. https://doi.org/10.1002/jps.22496
20. Cui, Z., Ni, N. C., Wu, J., Du, G. Q., He, S., Yau, T. M., Weisel, R. D., Sung, H. W., & Li, R. K. (2018). Polypyrrole-chitosan conductive biomaterial synchronizes cardiomyocyte contraction and improves myocardial electrical impulse propagation. Theragnostic, 8(10), 2752–2764. https://doi.org/10.7150/thno.22599
21. El-Schich, Z., Zhang, Y., Feith, M., Beyer, S., Sternbæk, L., Ohlsson, L., … Wingren, A. G. (2020). Molecularly imprinted polymers in biological applications. BioTechniques, 69(6), 406–419. https://doi.org/10.2144/btn-2020-0091
22. Farzin, A., Etesami, S. A., Quint, J., Memic, A., & Tamayol, A. (2020). Magnetic nanoparticles in cancer therapy and diagnosis. Advanced Healthcare Materials, 9(12), 1901058. https://doi.org/10.1002/adhm.201901058
23. Fefer, M., & Liu, J. (2016). Herbicidal composition with increased herbicidal efficacy. Google Patents.
24. Fresco-Cala, B., Batista, A. D., & Cárdenas, S. (2020). Molecularly imprinted polymer micro- and nanoparticles: A review. Molecules, 25(20), 4740. https://doi.org/10.3390/molecules25204740

25. Gao, R., Cao, B., Hu, Y., Feng, Z., Wang, D., Hu, W., … et al. (2013). Human infection with a novel avian-origin influenza A (H7N9) virus. The New England Journal of Medicine, 368(20), 1888–1897.
26. Garnier, M., Sabbah, M., Ménager, C., & Griffete, N. (2021). Hybrid molecularly imprinted polymers: The future of nanomedicine? Nanomaterials, 11(11), 3091. https://doi.org/10.3390/nano11113091
27. Ge, Y.-H., Shu, H., Xu, X.-Y., Guo, P.-Q., Liu, R.-L., Luo, Z.-M., … Fu, Q. (2019). Combined magnetic porous molecularly imprinted polymers and deep eutectic solvents for efficient and selective extraction of aristolochic acid I and II from rat urine. Materials Science and Engineering: C, 97, 650–657. https://doi.org/10.1016/j.msec.2018.12.057
28. Gidwani, B., & Vyas, A. (2015). A comprehensive review on cyclodextrin-based carriers for delivery of chemotherapeutic cytotoxic anticancer drugs. BioMed Research International, 2015, 198268. https://doi.org/10.1155/2015/198268
29. GLOBOCAN. (2020). New global cancer data. UICC. https://www.uicc.org/news/globocan-2020-new-global-cancer-dat
30. Hanahan, D., & Weinberg, R. A. (2011). Hallmarks of cancer: The next generation. Cell, 144(5), 646–674. https://doi.org/10.1016/j.cell.2011.02.013
31. Heidel, J. D., & Schluep, T. (2012). Cyclodextrin-containing polymers: Versatile platforms of drug delivery materials. Journal of Drug Delivery, 2012, 262731. https://doi.org/10.1155/2012/262731
32. Huang, H., Du, M., Chen, J., Zhong, S., & Wang, J. (2020). Preparation and characterization of abalone shells derived biological mesoporous hydroxyapatite microspheres for drug delivery. Materials Science and Engineering: C, 113, 110969. https://doi.org/10.1016/j.msec.2020.110969
33. Huang, J., Liu, H., Men, H., Zhai, Y., Xi, Q., & Zhang, Z. (2013). Molecularly imprinted polymer coating with fluorescence on a magnetic particle. Macromolecular Research, 21, 1021–1028.
34. Ishikawa, M., Yoshii, H., & Furuta, T. (2005). Interaction of modified cyclodextrins with cytochrome P-450. Bioscience, Biotechnology, and Biochemistry, 69(1), 246–248. https://doi.org/10.1271/bbb.69.246
35. Jiang, M., Ouyang, H., Ruan, P., Zhao, H., Pi, Z., Huang, S., Yi, P., & Crepin, M. (2011). Chitosan derivatives inhibit cell proliferation and induce apoptosis in breast cancer cells. *Anticancer Research, 31*(4), 1321–1328. [PubMed] [Google Scholar]
36. Jiang, Z., Han, B., Li, H., Yang, Y., Liu, W. (2015). Carboxymethyl chitosan represses tumor angiogenesis in vitro and in vivo. *Carbohydrate Polymers, 129*, 1–8. https://doi.org/10.1016/j.carbpol.2015.04.040 [PubMed] [Google Scholar]
37. Kaur, J., Gulati, M., Jha, N. K., Disouza, J., Patravale, V., Dua, K., Singh, S. K. (2022). Recent advances in developing polymeric micelles for treating cancer: Breakthroughs and bottlenecks in their clinical translation. *Drug Discovery Today, 27*(6), 1495–1512.
38. Kempe, H., Pujolràs, A. P., & Kempe, M. (2015). Molecularly imprinted polymer nanocarriers for sustained release of erythromycin. *Pharmaceutical Research, 32*(2), 375– 388.
39. Latchman, J., Guastella, A., & Tofthagen, C. (2014). 5-Fluorouracil toxicity and dihydropyrimidine dehydrogenase enzyme: Implications for practice. *Clinical Journal of Oncology Nursing, 18*(5), 581–

585. https://doi.org/10.1188/14.cjon.581-585

40. Lee, S., Miyajima, T., Sugawara-Narutaki, A., Kato, K., & Nagata, F. (2021). Development of paclitaxel-loaded poly (lactic acid)/hydroxyapatite core–shell nanoparticles as a stimuli- responsive drug delivery system. *Royal Society Open Science, 8*(12), 202030. https://doi.org/10.1098/rsos.202030 [PMC free article] [PubMed] [Google Scholar]
41. Li, J., Ying, S., Ren, H., Dai, J., Zhang, L., Liang, L., Wang, Q., Shen, Q., & Shen, J. W. (2020). Molecular dynamics study on the encapsulation and release of anti-cancer drug doxorubicin by chitosan. *International Journal of Pharmaceutics, 580*, 119241. https://doi.org/10.1016/j.ijpharm.2020.119241 [PubMed] [Google Scholar]
42. Li, S., Zhang, L., Zhang, H., Mu, Z., Li, L., & Wang, C. (2017). Rationally designed calcium phosphate/small gold nanorod assemblies using poly(acrylic acid calcium salt) nanospheres as templates for chemo-photothermal combined cancer therapy. *ACS Biomaterials Science & Engineering, 3*(9), 3215–3221. https://doi.org/10.1021/acsbiomaterials.7b00612 [PubMed] [Google Scholar]
43. Li, Z., Qin, C., Li, D., Hou, Y., Li, S., & Sun, J. (2014). Molecularly imprinted polymer for specific extraction of hypericin from *Hypericum perforatum* L. herbal extract. *Journal of Pharmaceutical and Biomedical Analysis, 98*, 210–220.
44. Loftsson, T., & Brewster, M. E. (2010). Pharmaceutical applications of cyclodextrins: Basic science and product development. *Journal of Pharmacy and Pharmacology, 62*(11), 1607– 1621. https://doi.org/10.1111/j.2042-7158.2010.01030.x [PubMed] [Google Scholar]
45. Ma, R.-T., & Shi, Y.-P. (2015). Magnetic molecularly imprinted polymer for the selective extraction of quercetagetin from *Calendula officinalis* extract. *Talanta, 134*, 650–656.
46. Mandal, A. K. (2021). Dendrimers in targeted drug delivery applications: A review of diseases and cancer. *International Journal of Polymeric Materials and Polymer Biomaterials, 70*(5), 287–297. https://doi.org/10.1080/00914037.2020.1713780 [Google Scholar]
47. Mavrikou, S., Tsekouras, V., Karageorgou, M.-A., Moschopoulou, G., & Kintzios, S. (2019). Detection of superoxide alterations induced by 5-fluorouracil on HeLa cells with a cell-based biosensor. *Biosensors, 9*(4), 126. https://doi.org/10.3390/bios9040126
48. Negm, N. A., Hefni, H. H. H., Abd-Elaal, A. A. A., Badr, E. A., & Abou Kana, M. T. H. (2020). Advancement on modification of chitosan biopolymer and its potential applications. *International Journal of Biological Macromolecules, 152*, 681–702. https://doi.org/10.1016/j.ijbiomac.2020.02.196 [PubMed] [Google Scholar]
49. Öpik, A., Menaker, A., Reut, J., & Syritski, V. (2009). Molecularly imprinted polymers: A new approach to the preparation of functional materials. *Proceedings of the Estonian Academy of Sciences, 58*(1), 3–11.
50. Park, E. K., Lee, S. B., & Lee, Y. M. (2005). Preparation and characterization of methoxy poly (ethylene glycol)/poly(ε-caprolactone) amphiphilic block copolymeric nanospheres for tumor-specific folate-mediated targeting of anticancer drugs. *Biomaterials, 26*(7), 1053– 1061.

51. Parker, R. M., Ratzan, S. C., & Lurie, N. (2003). Health literacy: A policy challenge for advancing high-quality health care. *Health Affairs, 22*(1), 147–153.
52. Qiu, N., Cai, L., Wang, W., Wang, G., Cheng, X., Xu, Q., Wen, J., Liu, J., Wei, Y., & Chen L. (2015). Barbigerone-in-hydroxypropyl-β-cyclodextrin-liposomal nanoparticle: Preparation, characterization and anti-cancer activities. *Journal of Inclusion Phenomena and Macrocyclic Chemistry, 82*(1), 505–514. https://doi.org/10.1007/s10847-015-0533-8 [Google Scholar]
53. Qiu, N., Li, X., & Liu, J. (2017). Application of cyclodextrins in cancer treatment. *Journal of Inclusion Phenomena and Macrocyclic Chemistry, 89*(3), 229–246. https://doi.org/10.1007/s10847-017-0752-2 [Google Scholar]
54. Ram Prasad, S., Jayakrishnan, A., & Sampath Kumar, T. S. (2019). Hydroxyapatite-poly (vinyl alcohol) core-shell nanoparticles for dual delivery of methotrexate and gemcitabine for bone cancer treatment. *Journal of Drug Delivery Science and Technology, 51*, 629–638. https://doi.org/10.1016/j.jddst.2019.03.041 [Google Scholar]
55. Rostami, E. (2020). Progresses in targeted drug delivery systems using chitosan nanoparticles in cancer therapy: A mini-review. *Journal of Drug Delivery Science and Technology, 58*, 101813. https://doi.org/10.1016/j.jddst.2020.101813 [Google Scholar]
56. Rosebrock, A. (n.d.). *Lesson sample: Advanced contour properties*. PyImageSearch. Retrieved May 18, 2025, from https://customers.pyimagesearch.com/lesson-sample- advanced-contour-properties/
57. Saraf, S., Jain, A., Tiwari, A., Verma, A., Panda, P. K., & Jain, S. K. (2020). Advances in liposomal drug delivery to cancer: An overview. *Journal of Drug Delivery Science and Technology, 56*, 101549. https://doi.org/10.1016/j.jddst.2020.101549 [Google Scholar]
58. Shakil, M. S., Mahmud, K. M., Sayem, M., Niloy, M. S., Halder, S. K., Hossen, M. S., Uddin, M. F., & Hasan, M. A. (2021). Using chitosan or chitosan derivatives in cancer therapy. *Polysaccharides, 2*(4), 795–816. https://doi.org/10.3390/polysaccharides2040048 [Google Scholar]
59. Sharma, V. K., Liu, X., Oyarzún, D. A., Abdel-Azeem, A. M., Atanasov, A. G., Hesham, A. E.-L., Barik, S. K., Gupta, V. K., & Singh, B. N. (2021). Microbial polysaccharides: An emerging family of natural biomaterials for cancer therapy and diagnostics. In *Seminars in Cancer Biology* (pp. 1–14). Academic Press. Cambridge, MA, USA. [DOI] [PubMed] [Google Scholar]
60. Siddique, S., & Chow, J. C. L. (2020). Gold nanoparticles for drug delivery and cancer therapy. *Applied Sciences, 10*(11), 3824. https://doi.org/10.3390/app10113824 [Google Scholar]
61. Sonnenschein, C., & Soto, A. M. (2020). Over a century of cancer research: Inconvenient truths and promising leads. *PLoS Biology, 18*(3), e3000670. https://doi.org/10.1371/journal.pbio.3000670 [PMC free article] [PubMed] [Google Scholar
62. Swaminathan, S., Cavalli, R., & Trotta, F. (2016). Cyclodextrin-based nanosponges: A versatile platform for cancer nanotherapeutics development. *Wiley Interdisciplinary Reviews: Nanomedicine and Nanobiotechnology, 8*(5), 579–601. https://doi.org/10.1002/wnan.1384 [PubMed] [Google Scholar]

63. Settle, J. (1998). Introduction and general overview of cyclodextrin chemistry. *Chemical Reviews, 98*(5), 1743–1754. https://doi.org/10.1021/cr970022c [PubMed] [Google Scholar]
64. Szejtli, J., & Osa, T. (1996). Volume 3. Cyclodextrins. In J. L. Atwood & J. M. Lehn (Eds.), *Comprehensive Supramolecular Chemistry* (pp. 1–52). Pergamon Press. New York, NY, USA. [Google Scholar]
65. Tang, H., Zhu, L., Yu, C., & Shen, X. (2012). Selective photocatalysis mediated by magnetic molecularly imprinted polymers. *Separation and Purification Technology, 95*, 165–171. https://doi.org/10.1016/j.seppur.2012.02.018
66. Tian, B., Hua, S., & Liu, J. (2020). Cyclodextrin-based delivery systems for chemotherapeutic anticancer drugs: A review. *Carbohydrate Polymers, 232*, 115805. https://doi.org/10.1016/j.carbpol.2019.115805 [PubMed] [Google Scholar]
67. Vasapollo, G., Sole, R. D., Mergola, L., Lazzoi, M. R., Scardino, A., Scorrano, S., & Mele, G. (2011). Molecularly imprinted polymers: Present and future prospective. *International Journal of Molecular Sciences, 12*(9), 5908–5945. https://doi.org/10.3390/ijms12095908
68. Wu, S. W., Liu, X., Miller, A. L., Cheng, Y. S., Yeh, M. L., & Lu, L. (2018). Strengthening injectable thermo-sensitive NIPAAm-g-chitosan hydrogels using chemical cross-linking of disulfide bonds as scaffolds for tissue engineering. *Carbohydrate Polymers, 192*, 308–316. https://doi.org/10.1016/j.carbpol.2018.03.047 [PubMed] [Google Scholar]

Graph

Graph 1 is available in the Supplementary Files section.

Figures

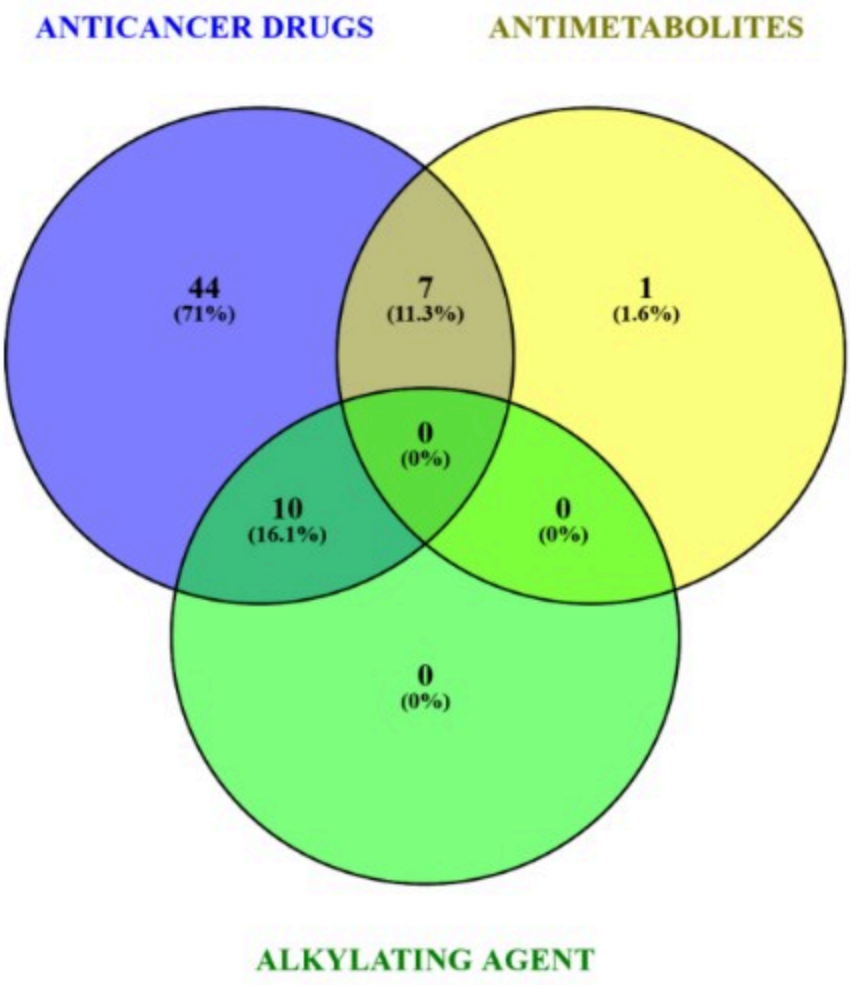


Figure 1

Represents the total number of anticancer drugs approved by the FDA in percentage.

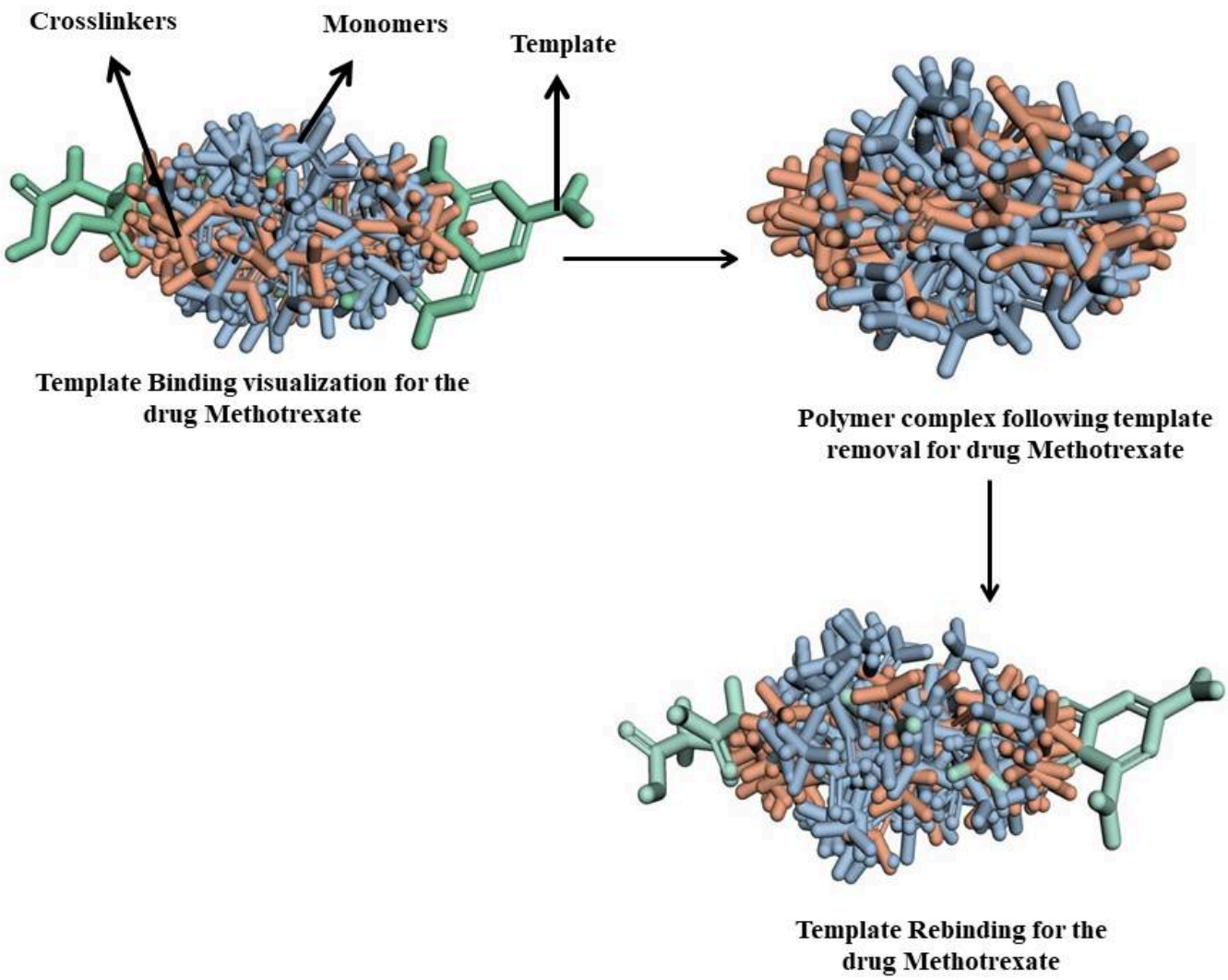


Figure 2

Template Binding, Removal and Rebinding visualization

for the drug Methotrexate

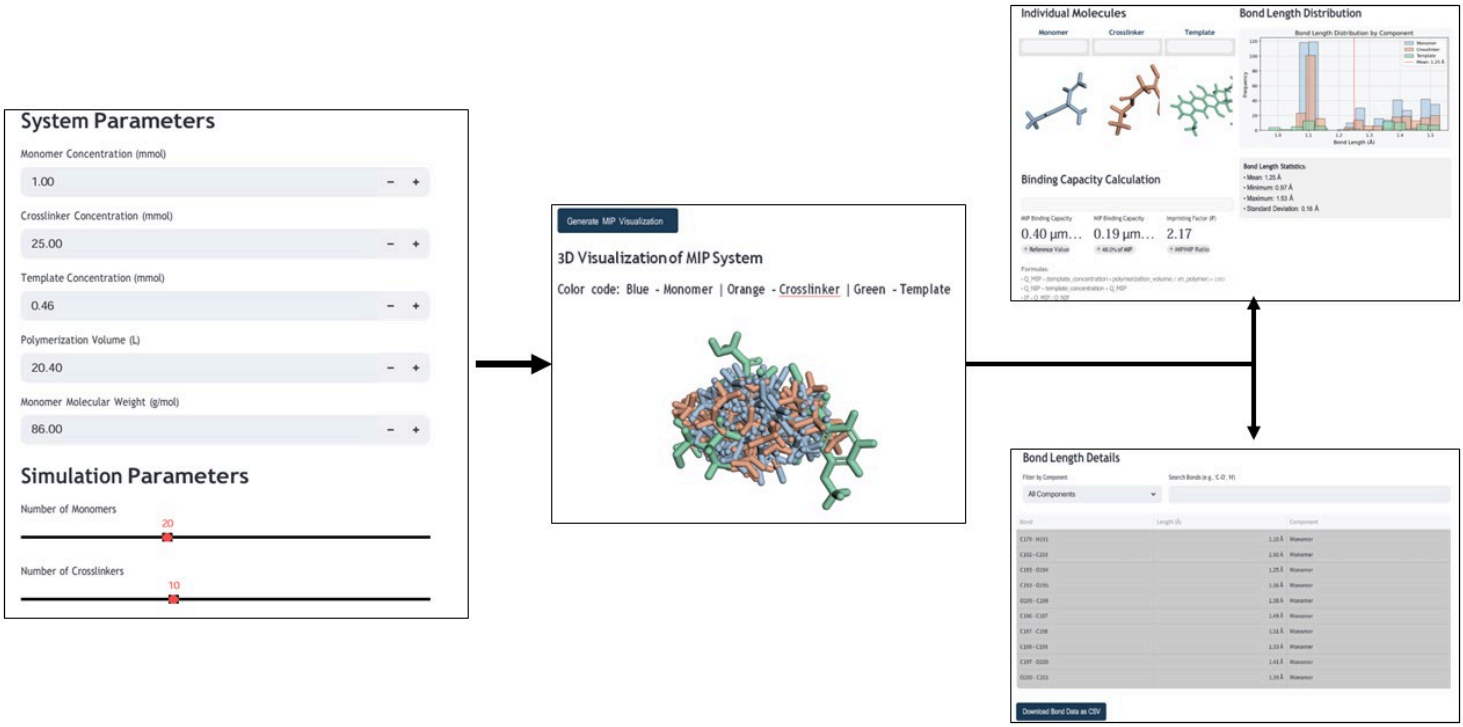


Figure 3

Represents the insights of the webserver for MIP system 3D visualization (hosted on streamlit).

Supplementary Files

This is a list of supplementary files associated with this preprint. Click to download.

- GAWebserver.jpg
- Figure4.jpg